COMPARISONS OF URBAN AND RURAL $PM_{10-2.5}$ AND $PM_{2.5}$ MASS CONCENTRATIONS AND SEMI-VOLATILE FRACTIONS IN NORTHEASTERN COLORADO

N. Clements[1], M.P. Hannigan[1], S.L. Miller[1], J.L. Peel[2], and J.B. Milford[1]

[1]{Department of Mechanical Engineering, College of Engineering and Applied Science, University of Colorado Boulder, Boulder, CO, 80309-0427}

[2]{Department of Environmental and Radiological Health Sciences, Colorado State University, Fort Collins, CO, 80523}

Correspondence to: N. Clements (nsclements@gmail.com)

Abstract

Coarse ($PM_{10-2.5}$) and fine ($PM_{2.5}$) particulate matter in the atmosphere adversely affect human health and influence climate. While $PM_{2.5}$ is relatively well studied, less is known about the sources and fate of $PM_{10-2.5}$. The Colorado Coarse Rural-Urban Sources and Health (CCRUSH) study measured $PM_{10-2.5}$ and $PM_{2.5}$ mass concentrations, as well as the fraction of semi-volatile material (SVM) in each size regime ($SVM_{2.5}$, $SVM_{10-2.5}$), from 2009 to early-2012 in Denver and comparatively rural Greeley, Colorado. Agricultural operations east of Greeley appear to have contributed to the peak $PM_{10-2.5}$ concentrations there, but concentrations were generally lower in Greeley than in Denver. Traffic-influenced sites in Denver had $PM_{10-2.5}$ concentrations that averaged from 14.6 to 19.7 μg/m^3 and mean $PM_{10-2.5}/PM_{10}$ ratios of 0.56 to 0.70, higher than at residential sites in Denver or Greeley. $PM_{10-2.5}$ concentrations were more temporally variable than $PM_{2.5}$ concentrations. Concentrations of the two pollutants were not correlated. Spatial correlations of daily averaged $PM_{10-2.5}$ concentrations ranged from 0.59 to 0.62 for pairs of sites in Denver and from 0.47 to 0.70 between Denver and Greeley. Compared to $PM_{10-2.5}$, concentrations of $PM_{2.5}$ were more correlated across sites within Denver and less correlated between Denver and Greeley. $PM_{10-2.5}$ concentrations were highest during the summer and early fall, while $PM_{2.5}$ and $SVM_{2.5}$ concentrations peaked in winter during periodic multi-day inversions. $SVM_{10-2.5}$ concentrations were low at all sites. Diurnal peaks in $PM_{10-2.5}$ and $PM_{2.5}$

concentrations corresponded to morning and afternoon peaks of traffic activity, and were enhanced by boundary layer dynamics. $SVM_{2.5}$ concentrations peaked around noon on both weekdays and weekends. $PM_{10-2.5}$ concentrations at sites located near highways generally increased with wind speeds above about 3 m s^{-1}. Little wind speed dependence was observed for the residential sites in Denver and Greeley. The mass concentration data reported here are being used in ongoing epidemiologic studies for PM in northeastern Colorado.

1 Introduction

Particulate matter (PM) in the troposphere is a complex mixture of inorganic and organic components with particle aerodynamic diameters ranging from a few nanometers to tens of micrometers. PM has been linked to multiple detrimental public health outcomes (U.S. EPA, 2004) and plays important roles in climatic processes including cloud formation (Wang et al., 2011), precipitation (Stevens and Feingold, 2009), and the solar radiation budget (Kim and Ramanathan, 2008). Particle size reflects emission sources and composition, with fine particulate matter ($PM_{2.5}$, aerodynamic diameters less than 2.5 µm) being derived primarily from combustion and industrial sources or produced through atmospheric processes (Seinfeld and Pandis, 2006). In contrast, coarse particulate matter ($PM_{10-2.5}$, aerodynamic diameters between 2.5 and 10 µm) is typically produced by abrasive processes or exists naturally, and is emitted from many different sources, often through suspension and dispersion (Minguillon et al., 2014). Particles commonly found in the coarse mode include geogenic mineral dust (Kavouras et al., 2007), vehicle-related emissions like road dust, brake-wear, and tire-wear particles (Harrison et al., 2012), particles emitted from industrial processes (Sawvel et al., 2015), sea-salt (Pakbin et al., 2011), road-salt (Kumar et al., 2012), microbiological organisms and their byproducts (Bowers et al., 2013, O'Sullivan et al., 2015), and organic matter from a variety of sources (Hiranuma et al., 2011; Cheung et al., 2012). $PM_{10-2.5}$ is expected to be mainly composed of non-volatile material, but this assumption has not been well studied. Due to the relatively short atmospheric lifetime of $PM_{10-2.5}$ and the wide range of potential local sources, $PM_{10-2.5}$ composition is typically heterogeneous across different ecological regions (Malm et al., 2007) and within urban areas (Cheung et al., 2011). $PM_{10-2.5}$ is poorly modeled using the Community Multiscale Air Quality (CMAQ) modeling system, suggesting both emissions and transport of this pollutant are not well understood and/or parameterized (Li et al., 2013).

In their review of the epidemiologic literature on the health risks of $PM_{2.5}$ and $PM_{10\text{-}2.5}$, Brunekreef and Forsberg (2005) concluded both fractions are harmful to human health. $PM_{2.5}$ consistently showed a significant relationship with mortality after adjustment for confounding pollutants. $PM_{10\text{-}2.5}$ showed inconsistent relationships with risk of mortality, though the reviewers concluded that $PM_{10\text{-}2.5}$ may have a stronger short-term effect than $PM_{2.5}$ for some endpoints like asthma and respiratory hospital admissions. A recent meta-analysis and review of epidemiologic studies of $PM_{10\text{-}2.5}$ health outcomes found evidence of increased risk of respiratory and cardiovascular morbidity and mortality with short-term increases in $PM_{10\text{-}2.5}$ concentrations (Adar et al., 2014). Long-term associations between $PM_{10\text{-}2.5}$ and health outcomes were not significant after accounting for the effects of $PM_{2.5}$. As highlighted by Wilson et al. (2005) and Adar et al., (2014), epidemiologic studies focusing on $PM_{10\text{-}2.5}$ must address the issue of spatial heterogeneity for proper health outcome and exposure assessment.

The Colorado Coarse Rural-Urban Sources and Health (CCRUSH) study aimed to compare the mass concentrations and composition of $PM_{10\text{-}2.5}$ in two distinctly different cities, Denver and Greeley, CO (Clements et al., 2012; Clements, 2013). To accomplish this objective, continuous $PM_{10\text{-}2.5}$ and $PM_{2.5}$ mass concentrations were measured for just over three years (Jan. 2009 - Apr. 2012), with a year of $PM_{10\text{-}2.5}$ and $PM_{2.5}$ filter samples collected every sixth day for compositional analyses (Feb. 2010 - Mar. 2011). Mass concentration results from the first year of the study were presented in Clements et al. (2012). Clements et al. (2014) presented results of trace element analysis of the filter samples. Bowers et al. (2013) presented an analysis of the bacterial community structure and diversity of the same filter set. This paper examines the full three-year data set for $PM_{10\text{-}2.5}$ and $PM_{2.5}$ mass concentrations and their semi-volatile fractions, which will be used in ongoing epidemiologic studies comparing urban and rural health effects of $PM_{10\text{-}2.5}$.

The particulate monitor used in the CCRUSH study, the tapered element oscillating microbalance (TEOM) model 1405-DF, is a semi-continuous dichotomous sampler that measures $PM_{10\text{-}2.5}$ and $PM_{2.5}$ directly with the inclusion of a virtual impactor (VI) after the PM_{10} inlet. The TEOM 1405-DF also quantifies the loss of semi-volatile material (SVM) from heated collection filters, providing total and semi-volatile mass concentrations on an hourly-average basis. 'Semi-volatile,' in the context of the TEOM instrument measurements, is defined as any particulate-bound substance that will evaporate at temperatures up to 30°C. Ammonium nitrate and semi-volatile organic compounds have been shown to comprise the majority of the semi-volatile mass lost from TEOM filter surfaces at 30°C (Grover et al., 2006).

This paper explores the factors that drove temporal and spatial variability of $PM_{10-2.5}$ and $PM_{2.5}$ total and semi-volatile concentrations during the CCRUSH study, focusing on how they differed across comparatively rural and urban sites. Temporal variability was assessed on multiple timescales, revealing the seasonal impacts of meteorology on particulate concentrations and the impact of traffic on diurnal pollutant profiles. Nonparametric regression analysis was used to explore the relationships between meteorological variables and $PM_{10-2.5}$ mass concentrations. Dynamics of relationships between $PM_{10-2.5}$ concentrations, traffic patterns, wind conditions, relative humidity (RH), and soil moisture were examined because these factors influence dispersion of dust from roadways and natural surfaces, an important emission pathway for $PM_{10-2.5}$ in the semi-arid western United States.

2 Materials and methods

2.1 Monitoring sites

CCRUSH study monitoring took place at four elementary schools, two located in Denver and two in Greeley, the details of which are presented in Table 1. Data from two additional monitoring sites operated by the Colorado Department of Public Health and Environment (CDPHE), CAMP and Denver Municipal Animal Shelter (DMAS), were included to provide additional insight into spatial and temporal variations. Figure S1 in the supplemental information provides a map of the monitoring sites. Denver is the largest city in Colorado and in 2011 had an estimated metropolitan-area population of 2,599,504, about half of the state population. Greeley is located 75 km north-northeast of Denver in Weld County and had a population of 95,357 in 2011 (U.S. Bureau of the Census, 2012). As of 2012, Weld County contained 2 million acres dedicated to farming and raising livestock (U.S. Department of Agriculture, 2012).

The two CCRUSH monitors in Denver were located at Alsup Elementary School (ALS) and Edison Elementary School (EDI). ALS is a residential-industrial site northeast of the urban core of Denver and about 4.5 km east of the intersection of four major roadways (I-25, I-270, I-76, and US-36). Interstate-76 is located a half kilometer away from ALS and runs diagonally from west to north of the site. A sand and gravel operation is located 0.5 km to the northwest. EDI is located in a residential area west of the urban core of Denver. The CDPHE sites CAMP and DMAS are located in downtown Denver and 5 km south of downtown, respectively. CAMP (AQS Site ID: 080310002) is a stand-alone building containing monitoring instruments for multiple pollutants. DMAS (AQS Site ID: 080310025) was part of the EPA NCore Multipollutant Monitoring Network and was located on the rooftop of the Denver Municipal Animal Shelter, 0.1 km west of I-25. The two CCRUSH sites in Greeley were located in residential areas, with McAuliffe Elementary School (MCA) located on the west side of town in the suburban fringe and Maplewood Elementary (MAP) located nearer to the town center. A summary of traffic levels for major roadways near all sites is included in Table S1. The two major roadways near Greeley, US-85 and US-34, had an order of magnitude less traffic per hour than the interstates in Denver and are located 2.7 km east and 3.1 km south of MAP, respectively.

2.2 Particulate matter monitoring

A TEOM 1405-DF (Thermo Scientific Inc.) semi-continuous particulate monitor was operated at each CCRUSH site for three years, with the exception of MCA, where the TEOM was only operated for six months before being shut down due to a leak in the instrument's Filter Dynamic Measurement System (FDMS) linear-valve seals. The TEOM quantifies particulate concentrations by measuring changes in the oscillating frequency of a tapered glass element as particles are deposited on a filter placed on the tip of the element. Oscillating frequency is converted to deposited mass via a calibration coefficient and first principles (Thermo Scientific, 2009). All monitors were placed in temperature-controlled shelters on school rooftops with the exception of MCA, where the monitor was placed in an attic with inlet tubing running through the ceiling onto the rooftop. At monthly intervals, all TEOM monitors were thoroughly cleaned and inspected, TEOM (TEOM TX40, Thermo Scientific) and FDMS (47mm TX40, Thermo Scientific) filters were changed, and flow rates were calibrated. Data were downloaded during each monthly visit and processed on-site to further identify possible instrument issues. Sites were visited every one to two weeks for general instrument inspection, performing flow audits, and to observe and log instrument conditions. All TEOM 1405-DF instruments were operated and maintained according to the manufacturer's specifications. Raw mass concentrations based on actual sample flow rates, which contain no interpolated values, were downloaded and corrected for the deposition of $PM_{2.5}$ in the $PM_{10-2.5}$ channel due to the VI. Prior publications from the CCRUSH study present further data processing details (Clements et al., 2012; Clements et al., 2013).

The TEOM 1405-DF quantifies concentrations of semi-volatile species with the use of the FDMS, which consists of a linear valve that diverts the sample flow to chilled FDMS filters (4°C), cleaning the sample stream. At six-minute intervals the FDMS valve changes position, switching between depositing sample particles on TEOM filters and flowing clean air across TEOM filters. TEOM filter mass change measured during the particle depositing mode measures the non-volatile particulate mass, and the mass change when clean air is flowing through collection filters measures the loss of semi-volatile mass due to the heated TEOM filters (30°C, Hering et al., 2004). Summing the two fractions gives the total particulate mass concentration. Hourly and daily averages of $PM_{2.5}$ and $PM_{10-2.5}$ total, non-volatile, and semi-volatile mass concentrations were calculated from the raw six-minute data for the CCRUSH data set. Hourly and daily averages missing more than 25% of the data from the specified time interval were censored due to lack of completeness.

Quality checked hourly-average PM_{10} and $PM_{2.5}$ total mass concentration data were provided by the CDPHE for the CAMP and DMAS monitoring sites. At both sites, a PM_{10} TEOM without FDMS and a $PM_{2.5}$ TEOM with FDMS were collocated on site rooftops. CDPHE $PM_{10-2.5}$ concentrations were estimated by subtracting $PM_{2.5}$ from PM_{10} mass concentrations. PM_{10} concentrations, and subsequently $PM_{10-2.5}$ concentrations, were not available from CAMP from 1/1/2009 to 11/19/2010 due to a data logging issue with the TEOM. Due to the errors that are introduced by the subtraction-method when using a combination of TEOMs with and without semi-volatile mass loss correction, daily average CDPHE data containing this error were corrected following the methods of Clements et al. (2013). This correction estimated the daily average semi-volatile fraction of $PM_{2.5}$ ($SVM_{2.5}$) from total $PM_{2.5}$ concentrations for the CAMP and DMAS time series using linear regression. Nine months of $SVM_{2.5}$ and $PM_{2.5}$ data collected at each site from October 2011 through July 2012 were used to develop the correction models at each site. Daily mean $SVM_{2.5}$ concentrations measured at CAMP and DMAS during this period were 1.62 and 2.95 $\mu g/m^3$, respectively. Resulting estimates of $SVM_{2.5}$ concentrations from linear regression during the CCRUSH campaign were 1.46 and 2.72 $\mu g/m^3$ at CAMP and DMAS, respectively. Modeled $SVM_{2.5}$ concentrations were subtracted from total $PM_{2.5}$ concentrations, yielding nonvolatile $PM_{2.5}$ concentrations that were then subtracted from measurements from the collocated PM_{10} TEOM monitor to estimate $PM_{10-2.5}$. Due to the very low concentrations of $PM_{10-2.5}$ SVM ($SVM_{10-2.5}$) in Colorado, this correction method was shown to closely estimate true $PM_{10-2.5}$ concentrations. Hourly averaged $PM_{10-2.5}$ concentrations could not be corrected due to the low coefficients of determination for the $SVM_{2.5}$ vs. $PM_{2.5}$ linear regression relationships at CAMP and DMAS. Uncorrected CDPHE $PM_{10-2.5}$ hourly mass concentrations may be biased by up to 30%, on average. Such errors have been shown to affect both spatial and temporal summary statistics (Clements et al., 2013).

2.3 Meteorology, gas-phase pollutant, and traffic count data

Ambient temperature and RH were measured by each TEOM throughout the CCRUSH campaign. Relative humidity data from ALS were used for comparison with pollutant concentration data from CAMP and DMAS. Additional meteorological data collected by the CDPHE include ambient temperature and wind conditions at CAMP; temperature and wind at DMAS; wind at ALS; and wind at Carriage (CRG), a site 1.75 km southeast of EDI. CRG wind data were used for comparisons with EDI pollutant concentration data. Winds were measured at 10.5 m at all sites except ALS, which had a 14.0 m tower. Ambient temperature, RH, and wind condition data sets were downloaded from the National Climatic Data Center for the Greeley Airport (GREA) site operated by NOAA (Site #: 24051/GXY). Soil moisture data were downloaded for the Nunn #1 site (NUN, SCAN Site #: 2017) located in Weld County and operated by the United States Department of Agriculture's National Resources Conservation Service. Soil moisture data are compared to pollutant concentration data collected in Greeley. From this set of meteorological variables, hourly and daily arithmetic averages were calculated for ambient temperature, RH, and soil moisture. Vector averages were calculated for wind conditions.

CDPHE also provided gas-phase pollutant data from CAMP (NO, SO_2, CO), DMAS (O_3, NO, SO_2, CO), GRET (O_3, CO) and Welby (WBY) a site 1.5 km northwest of ALS located on the northwest side of I-76 (O_3, NO, SO_2, CO). Hourly vehicle count data were downloaded from the Colorado Department of Transportation Data Explorer for I-25, I-70, I-76, and I-270 in Denver, and CO-257 and US-85 in Greeley. Traffic count site details and distances to nearest CCRUSH monitoring sites can be found in Table S1. When calculating correlations between particulate data and the meteorological, gas-phase pollutant, and traffic data, site pairs that are nearest to each other were compared.

2.4 Data analysis

In addition to standard descriptive statistics, the concordance correlation coefficient (CCC) and coefficient of divergence (COD) were used to compare air pollutant time series. The concordance correlation coefficient (CCC) accounts for correlation as well as divergence from the concordance, or 1:1 line, and is a measure of reproducibility (Lin, 1989). The CCC is useful in quantifying the spatial homogeneity of a pollutant, and can be compared to the Pearson's correlation coefficient, ρ, directly through a bias correction factor (C_b), as shown in equation 1. For time series from sites *j* and *h*, σ_j^2 and σ_h^2 are time series variances, σ_{jh} is the covariance, and μ_j and μ_h are mean values.

$$CCC = \frac{2\sigma_{jh}}{\sigma_j^2+\sigma_h^2+(\mu_j-\mu_h)^2} = \rho C_b \tag{1}$$

A common measure of spatial homogeneity, the coefficient of divergence (COD, equation 2), is also considered for comparison with other studies. In calculating the COD, X_{ij} and X_{ih} represent measurement *i* from monitoring sites *j* and *h*, respectively, and *n* is the total number of data points considered.

$$COD = \sqrt{\frac{1}{n}\sum_{i=1}^{n}\left(\frac{X_{ij}-X_{ih}}{X_{ij}+X_{ih}}\right)^2} \tag{2}$$

Correlation analysis was performed between particulate and meteorological, gas-phase pollutant, and traffic data. A summary of these results is included in Table S2 of the supplemental information. $PM_{2.5}$ was moderately correlated with gas-phase species and negatively correlated with wind speed. $PM_{10-2.5}$ was correlated with both traffic and RH, but no linear relationship was observed with wind speed. To further investigate trends observed in the correlation analysis, nonparametric regression (NPR) was used to compare pollutant concentrations and meteorological conditions important for dust emissions (wind speed, wind direction, RH, and soil moisture) using the methods described in Clements et al. (2012). This approach provides objectively smoothed estimates of the expected value of the concentration as a function of the explanatory variable. The Nadaraya-Watson estimator is used to calculate weighted average concentrations within a moving window:

$$C(\theta) = \frac{\sum_{i=1}^{n} K\left(\frac{\theta-W_i}{\Delta\theta}\right)C_i}{\sum_{i=1}^{n} K\left(\frac{\theta-W_i}{\Delta\theta}\right)} \tag{3}$$

where θ is the value of the explanatory variable for which the estimate is made, W_i is the value of the explanatory variable at time i, $\Delta\theta$ is the smoothing parameter, and K references the averaging kernel. A Gaussian kernel was applied to all meteorological NPRs. Wind speed and direction regressions excluded "calm" conditions, approximated as hours with wind speeds below 0.5 m/s. An optimal smoothing parameter for each meteorological variable and pollutant type was determined via leave-one-out cross validation (Henry et al., 2002). For each meteorological variable and pollutant pair considered, the optimal smoothing parameters from all sites were averaged together and this average smoothing parameter was used to assess final NPR relationships. Smoothing parameters used for $PM_{10-2.5}$ were: 0.32 m/s for wind speed, 9.3° for wind direction, 3.25% for RH, and 0.30% for soil moisture (MAP only). Smoothing parameters used for $PM_{2.5}$ were: 0.24 m/s for wind speed, 6.7° for wind direction, 1.65% for RH, and 0.30% for soil moisture (MAP only). NPR results for wind speeds above the 99.9th percentile for each site are not displayed due to limited data coverage and high uncertainties in those regions of the regressions. Ninety-five percent confidence intervals of nonparametric regressions were calculated using the methods of Henry et al. (2002). Kernel-smoothed hourly-average pollutant and meteorological time series are also presented using a smoothing factor of three hours.

3 Results and Discussion

3.1 Summary statistics

Table 2 gives a statistical summary of the daily average particulate matter concentration data. The highest mean $PM_{2.5}$ concentrations were measured at DMAS (10.15 μg/m^3) and ALS (9.02 μg/m^3). Both of these sites were located in semi-industrial parts of Denver and were less than 0.5 km from interstate highways. The lowest average $PM_{2.5}$ mass concentrations were measured east of downtown Denver at the residential site, EDI. The average Denver $PM_{2.5}$ mass concentration over the whole CCRUSH campaign was 8.74 μg/m^3, which is similar to the average $PM_{2.5}$ concentration of 8.42 μg/m^3 measured in Greeley.

Average $PM_{10-2.5}$ concentrations showed a different spatial pattern from $PM_{2.5}$. Average $PM_{10-2.5}$ concentrations at CAMP (19.71 μg/m^3), ALS (15.30 μg/m^3), and DMAS (14.60 μg/m^3) were elevated substantially above concentrations measured at EDI (8.02 μg/m^3). Nearby interstate highways likely contributed to the relatively high $PM_{10-2.5}$ concentrations measured at ALS and

DMAS. Downtown traffic on nearby roads within 20 m of all sides of CAMP was a likely local $PM_{10-2.5}$ source at that location. The average $PM_{10-2.5}$ concentrations at the MAP and MCA sites in Greeley were 10.34 µg/m^3 and 9.87 µg/m^3, respectively, falling between the concentrations measured at EDI and at the traffic-influenced sites in Denver. Ninety-fifth percentile values of $PM_{10-2.5}$ were roughly double those for $PM_{2.5}$, with the traffic-influenced sites having the highest peak concentrations. Like the mean values, 95th percentile values of $PM_{10-2.5}$ at the Greeley sites fell between those at EDI and those at the traffic-influenced sites in Denver. For the CCRUSH sites, mean and 95th percentile concentration values for both $PM_{2.5}$ and $PM_{10-2.5}$ over the three-year period were similar to those observed during the first year (Clements et al., 2012).

Using data from co-located PM_{10} and $PM_{2.5}$ monitors that had been reported to the U.S. Environmental Protection Agency's Air Quality System (AQS), Li et al. (2013) estimated average $PM_{10-2.5}$ concentrations of 17.25 µg/m^3 for 50 sites across the western United States. Values in Denver and Greeley were similar to $PM_{10-2.5}$ concentrations in Seattle, WA (9.0 and 14.8 µg/m^3), Spokane, WA (15.9 µg/m^3), Salt Lake City, UT (11.1 and 12.7 µg/m^3), and multiple cities in California (e.g. San Diego, Sacramento, Anaheim, and Fresno). Sites located in the arid southwest (Arizona, New Mexico, and Texas) tended to have higher $PM_{10-2.5}$ concentrations due to geogenic dust emissions.

As shown in Table 2, the urban-residential site EDI and the two Greeley sites had the lowest average $PM_{10-2.5}/PM_{10}$ ratios (0.49 – 0.53). Among the traffic-influenced sites, ALS and DMAS had mean ratios of 0.59 and 0.56, respectively, while CAMP had a mean ratio of 0.70. CAMP is essentially a curbside monitor for local street traffic in downtown Denver. Liu and Harrison (2011) observed a similar gradient in $PM_{10-2.5}/PM_{10}$ ratios in the United Kingdom, with curbside and roadside monitors having the highest ratios (0.71 and 0.57 on average, respectively) and urban background or rural sites having the lowest ratios (0.54-0.51).

On a day-to-day basis $PM_{10-2.5}$ was generally more temporally variable than $PM_{2.5}$, with higher coefficients of variation (COV) and absolute standard deviations than $PM_{2.5}$ at all sites except at EDI, where $PM_{2.5}$ was more temporally variable than at all other sites (Table 2). Daily $PM_{10-2.5}$ COV were highest at ALS, MCA, and MAP, while the three traffic-influenced sites had the highest $PM_{10-2.5}$ standard deviations.

EDI, CAMP, and MAP had the lowest hourly $PM_{10-2.5}$ COVs of 0.96, 1.07 and 1.09, respectively. ALS, MCA and DMAS had higher hourly COV of 1.2, 1.28 and 1.34. As will be shown in the next section, traffic is highly influential in driving diurnal $PM_{10-2.5}$ variability, which is reflected in the increased COV for traffic-influenced sites at the hourly time-scale. The hourly COV for $PM_{10-2.5}$ for the sites in northeastern Colorado can be compared with those Li et al. (2013) estimated from co-located PM_{10} and $PM_{2.5}$ measurements across the western United States. They estimated COV for 25 sites with hourly data, which ranged from 0.7 to 2.0. Hourly COV for 13 of the 25 sites were above 1.5 (Li et al., 2013), so the temporal variability observed in northeastern Colorado generally falls at the lower end of the range they reported.

Semi-volatile concentrations were measured in both particle size ranges, though concentrations were low in the $PM_{10-2.5}$ range. Average $SVM_{2.5}$ concentrations ranged from 2.05 μg/m^3 at EDI to 2.58 μg/m^3 at MCA. $PM_{2.5}$ at the MAP site in Greeley contained 29% semi-volatile material on average, similar to percentages at Denver sites ALS (26%) and EDI (27%). Little to no seasonal variability was observed in the $SVM_{2.5}/PM_{2.5}$ ratios. For comparison, $PM_{2.5}$ at a background site in Paris, France was found to be 23% and 18% semi-volatile material in winter and summer, respectively, using TEOM instruments (Favez et al., 2007). Ammonium nitrate and semi-volatile organic matter were shown to explain the majority of $PM_{2.5}$ semi-volatile material as measured by TEOMs in Fresno, CA (Grover et al., 2006), Paris (Favez et al., 2007), and Beijing (Sciare et al., 2007).

The highest semi-volatile concentrations in the coarse size range were measured at ALS, averaging just 0.20 μg/m^3, about 1% of the total mass concentration average. Low semi-volatile concentrations in the coarse particle size range suggest that ammonium nitrate and semi-volatile organic matter are not found in large concentrations in the coarse mode at our study sites. Gas-phase nitric acid does partition to the coarse mode via heterogeneous reactions with dust-related minerals (Usher et al., 2003), but the reaction products are not volatile at 30°C. Mineral-bound nitrate is commonly measured in urban and rural coarse aerosols (Cheung et al., 2011; Lee et al., 2008). The slight signal in $SVM_{10-2.5}$ at ALS might be in part due to semi-volatile PAHs, which have been measured at traffic sites in the coarse mode in California (Cheung et al., 2012). Semi-volatile organic species have also been identified in the coarse mode during haze events in China (Wang et al., 2009).

3.2 Time series and monthly trends

Figure 1 shows smoothed ($\Delta\theta$ = 3 hours) time series of particulate mass concentrations, gas-phase pollutant concentrations, and meteorological conditions. To highlight the seasonal trends, monthly medians of daily average concentrations are presented in Figure S2 of the supplemental information. Monthly medians for $PM_{2.5}$ and $SVM_{2.5}$ show the same annual pattern, with a primary peak in winter and a smaller peak in the middle of summer. As expected, O_3 concentrations also peaked in summer, while CO and NO peaked in winter.

A recent source apportionment study in Denver found significant contributions to the $PM_{2.5}$ fraction from a light n-alkane/PAH factor during summer, which would contribute to the semi-volatile fraction measured by the TEOM during this time (Xie et al., 2013). The Denver Aerosol Sources and Health (DASH) study also found that $PM_{2.5}$ nitrate and organic species indicative of motor vehicle emissions peaked in Denver during winter (Dutton et al., 2010). These species are likely to have contributed to wintertime $PM_{2.5}$ and $SVM_{2.5}$ peaks in the CCRUSH study as well. Factor analysis of trace element data from 24-hour filter samples collected at the CCRUSH sites every sixth day from February 2010 – March 2011 showed a factor accounting for 80% of the sulfur contributing about 50 to 60% of the $PM_{2.5}$ trace element concentrations and peaking in winter and fall (Clements et al., 2014). Some wintertime $PM_{2.5}$ peaks appear to be due to episodic inversions, identified by simultaneous increases in CO and NO with peaks in both $PM_{2.5}$ and $SVM_{2.5}$. Wintertime inversions did not affect $PM_{10\text{-}2.5}$ to the same extent, as $PM_{10\text{-}2.5}$ concentrations decreased during many of the periods of high $PM_{2.5}$. Calm winds during multi-day inversions would inhibit resuspension, which may be why $PM_{10\text{-}2.5}$ concentrations are relatively low during these periods while $PM_{2.5}$ and gas-phase species build up.

Temporal trends in $PM_{10\text{-}2.5}$ are less obvious than those for $PM_{2.5}$ due to the relatively variable nature of $PM_{10\text{-}2.5}$ concentrations. As also reflected in the summary statistics, Figure 1 shows relatively large differences in $PM_{10\text{-}2.5}$ mass concentrations between sites compared to $PM_{2.5}$. The highest $PM_{10\text{-}2.5}$ concentrations were measured at CAMP during the summer and fall of 2011, though this monitoring site only operated through the second half of the CCRUSH study. For sites with multiple years of monitoring data, there were no pronounced differences in year-to-year average particulate concentrations or in year-to-year COVs.

As shown more distinctly in the monthly median plots in the supplemental information, $PM_{10\text{-}2.5}$ at most of the sites was highest in summer and fall. $PM_{10\text{-}2.5}$ at EDI was the exception, displaying relatively little seasonality. In the analysis of February 2010 – March 2011 trace element data from the CCRUSH filter samples, Clements et al. (2014) found that a factor associated with mineral dust contributed more than half of the trace element mass in $PM_{10\text{-}2.5}$, peaking in summer and fall when RH and soil moisture were low. Dry environmental conditions increase dust emissions from roads (Amato et al., 2014) and soil surfaces (Kim and Choi, 2015). Relative humidity was highest during winter and lowest in March and September, while wind speed was highest during spring, peaking in April.

3.3 Spatial comparisons

Spatial comparisons between each monitoring site for daily averaged $PM_{2.5}$, $SVM_{2.5}$, and $PM_{10-2.5}$ are presented in Table 3, including both pairwise correlation coefficients and CCC values. Bias correction factors (C_b) are listed in parentheses for comparisons between sites for the same pollutant. Correlation coefficients for $PM_{2.5}$ ranged from 0.65 for the ALS-EDI pair to 0.92 for CAMP-DMAS. $PM_{10-2.5}$ correlation coefficients for sites within Denver ranged from 0.59 for ALS-CAMP to 0.79 for CAMP-DMAS. Correlations for $PM_{10-2.5}$ between MAP and the Denver sites ranged from 0.47 for CAMP-MAP to 0.70 for ALS-MAP, whereas those for $PM_{2.5}$ ranged from 0.34 for EDI-MAP to 0.61 for ALS-MAP. Relatively high regional correlations for $PM_{10-2.5}$ suggest that weather patterns moving through region influence the temporal variability of this pollutant on daily timescales. Similar temporal variability of emission sources (e.g. traffic) could also contribute to high regional correlations for $PM_{10-2.5}$. Correlations within Greeley were also high; as reported by Clements et al. (2012) the correlation coefficients for $PM_{2.5}$ and $PM_{10-2.5}$ between MAP and MCA over six months of monitoring were 0.82 and 0.98, respectively. Lastly, spatial $SVM_{2.5}$ correlations for the CCRUSH sites were moderate, from 0.26 (MAP-EDI) to 0.53 (ALS-EDI).

Daily average $PM_{10-2.5}$ concentrations in Denver and the Front Range tended to be more spatially correlated than observed in previous studies using continuous monitors in Los Angeles, CA and the United Kingdom (Moore et al., 2010; Liu and Harrison, 2011). Li et al. (2013) found correlation values for $PM_{10-2.5}$ that were comparable to those in Colorado for four sites in El Paso, TX ($0.49<\rho<0.76$), two sites in Albuquerque, NM ($\rho=0.53$), three sites in North Dakota ($0.46<\rho<0.60$), and three sites in northern Idaho/northeastern Washington ($0.48<\rho<0.61$). For 24-hour $PM_{10-2.5}$ filter samples collected at 10 sites around the Los Angeles, CA metropolitan area, Pakbin et al. (2010) showed moderate to high correlation between urban Los Angeles sites ($0.48<\rho<0.80$) and lower correlations for an industrial shipping site ($0.04<\rho<0.25$), and semi-rural sites in Riverside ($0.04<\rho<0.48$).

The CCC represents correlation that has been penalized according to the mean difference in concentrations between two sites. For $PM_{2.5}$, comparisons between MAP and the Denver sites produced the lowest CCC values, corresponding to the low correlation coefficients for the same data comparisons. For $PM_{10-2.5}$, the lowest CCC and C_b values were for comparisons between CAMP and the other sites, corresponding to the relatively high concentrations observed at CAMP. Within Denver, concentrations of $PM_{10-2.5}$ were more heterogeneous than those for $PM_{2.5}$. Low to no correlation or concordance was found between $PM_{2.5}$ and $PM_{10-2.5}$ for all site pairs. COD values are presented in Table S3 and agree with the CCC results, showing $PM_{10-2.5}$ to be more spatially heterogeneous than $PM_{2.5}$.

Using nonparametric regression with wind direction, Clements et al. (2012) identified the influence of emissions from a sand and gravel operation less than 0.5 km west of ALS. Interstate-76 is also located nearby, about 0.5 km away in the same general direction. During the 3-year study period, average $PM_{10-2.5}$ concentrations at ALS exceeded 25 µg/m^3 when winds were from 225 to 315 degrees, compared to an average of about 13 µg/m^3 with winds from all other directions. Seasonal wind roses for ALS are shown in Figure S3 of the supplemental information. To determine how spatial correlations were affected by the local sources at ALS, hourly concentrations collected while wind was coming from 225 to 315 degrees were removed from the ALS time series. Daily averages were recalculated and one daily average value was removed due to having less than 75% of hourly values remaining. With the adjustment, the overall mean $PM_{10-2.5}$ concentration at ALS was reduced from 15.30 µg/m^3 to 14.38 µg/m^3. With the censored data, correlations for $PM_{10-2.5}$ at ALS with the other sites increased by 2% to 8%. CCC values were reduced by 4% for ALS-CAMP and increased by 11% to 19% for the other site comparisons, due mainly to the reduced mean concentration at ALS.

3.4 Diurnal and day of week trends

Figure 2 compares median pollutant concentrations and traffic counts for each hour of the day for weekdays and weekends. $PM_{2.5}$ peaked in the morning on weekdays, a trend that nearly disappeared on weekends. In contrast, $SVM_{2.5}$ generally peaked at noon on both weekdays and weekends, preceding the early afternoon ozone peak by about two hours. Bimodal diurnal profiles were observed on weekdays for $PM_{10-2.5}$ at all sites except ALS, with peaks in the morning (6:00-8:00 MT) and late afternoon (18:00-20:00 MT). The morning peak in $PM_{10-2.5}$ disappears on weekends, likely due to the absence of a morning traffic peak. Late afternoon $PM_{2.5}$ concentrations typically started increasing around 6:00 PM MT due to a lowering boundary layer, a trend that was accentuated in winter and fall. Peak $PM_{10-2.5}$ concentrations correspond well with this increase in $PM_{2.5}$, even though the peak in traffic occurred an hour earlier. Using the Kruskal-Wallis test with daily averages (5% significance level), it was determined that $PM_{10-2.5}$ concentrations were significantly higher on weekdays than weekends at all sites (all p-values < 0.05). $PM_{2.5}$ weekday-weekend comparisons showed significant differences only at ALS and CAMP (p-values of 0.02 for both locations).

3.5 Nonparametric Regression

Figures 3a and 3b present nonparametric regression results for $PM_{10-2.5}$ and $PM_{2.5}$ versus RH, showing that $PM_{10-2.5}$ decreased and $PM_{2.5}$ increased with increasing RH. Above 50% RH, $PM_{10-2.5}$ concentrations tended to decrease rapidly, generally dropping to below 5 µg/m^3 when RH levels were over 90%. Maximum $PM_{10-2.5}$ concentrations occurred for RH below 50% at all sites. At higher RH, surface wetting likely inhibits resuspension, thus suppressing $PM_{10-2.5}$ mass concentrations. In contrast, the increase in $PM_{2.5}$ mass concentrations with increased RH is likely due to hygroscopic growth and enhanced dissolution of water-soluble species.

As shown in Figures 3c and 3d, $PM_{2.5}$ and $PM_{10-2.5}$ concentrations also displayed contrasting relationships with wind speed. Regressions of $PM_{10-2.5}$ against wind speed at ALS, DMAS, and CAMP displayed a U-shaped profile, with concentrations decreasing for wind speeds up to 2 to 3 m/s, then increasing with wind speeds above 3 m/s. $PM_{10-2.5}$ at EDI does not appear to be sensitive to wind speed, though lower wind speeds in general were experienced at EDI (99.9th percentile less than 6 m/s). CAMP also experienced lower wind speeds, but displays a U-shaped profile, possibly due to resuspension of road dust. Wind speeds were highest in Greeley, but the average $PM_{10-2.5}$ concentration increased by only a few µg/m^3 as wind speeds increased from about 6 m/s to more than 10 m/s. $PM_{2.5}$ concentrations generally decreased as wind speeds increased, reflecting the effect of dilution. Studies in Europe have observed similar relationships between $PM_{10-2.5}$ and wind speed to those presented here, with most sites showing U-shaped relationships and sites located near sources showing more resuspension than background or residential sites (Harrison et al., 2001; Charron and Harrison, 2005; Liu and Harrison, 2011; Barmpadimos et al., 2012).

As shown in Figure 3e, $PM_{10-2.5}$ concentrations at MAP peaked with soil moisture levels below 13%, and decreased sharply with moisture levels above 25%. $PM_{2.5}$ concentrations decreased with soil moisture values above 30%. The highest soil moisture and RH levels were observed during precipitation or snowfall events (Figure 1), so the high ends of the RH (>80%) and soil moisture (>30%) regressions might partly reflect precipitation scavenging. Amato et al. (2013)

analyzed the effect of rain on non-exhaust traffic emissions and found that contributions from different sources (e.g. tire wear and road wear) recovered at different rates after precipitation events. Biological particles have also been shown to have complex relationships with precipitation, sometimes increasing in concentration during and immediately after rainfall (Huffman et al., 2013).

To separate the effects of RH and wind speed, additional NPRs for $PM_{10\text{-}2.5}$ against wind speed were assessed using data sets for ALS and MAP, sorted for RH above and below 50%. This threshold was chosen because of the significant decrease in average concentrations observed above 50% RH. Figure 3g shows that resuspension at ALS was heavily inhibited at elevated RH. In contrast, as shown in Figure 3h, $PM_{10\text{-}2.5}$ concentrations at MAP are higher at lower RH but exhibit relatively little dependence on wind speed at either low or high RH.

Wind direction NPRs for $PM_{10\text{-}2.5}$ and $PM_{2.5}$ are found in Figures 4 and 5, respectively. For both size ranges, wind direction trends for ALS and EDI in the three-year data set were similar to those identified by Clements et al. (2012) for the initial year of data. Results for $PM_{2.5}$ and $PM_{10\text{-}2.5}$ at MAP show greater differences. The wind direction regression for $PM_{10\text{-}2.5}$ at MAP shows increased concentrations with winds from the east to southeast and from the northwest. A local intersection is located 0.4 km to the northwest of MAP and might be a source of the northwesterly peak at this site. The more urban parts of Greeley and two large cattle feedlots are located to the southeast of MAP. Cow fecal matter was identified as a major contributor to $PM_{10\text{-}2.5}$ bacterial diversity throughout the year in Greeley (Bowers et al., 2013).

Winds from the south and west brought increased concentrations of $PM_{2.5}$ to MAP, which could be a result of nighttime downslope flow transporting urban aerosol generated in Denver and other Front Range communities. The increase with winds from the south and west does not appear in the $PM_{10\text{-}2.5}$ wind direction regression, although the northwesterly peak appears in regressions for both size regimes. The lack of a peak to the south or west in the NPR for $PM_{10\text{-}2.5}$ at MAP is consistent with the expectation that regional transport of $PM_{10\text{-}2.5}$ is limited by relatively rapid deposition rates.

$PM_{10\text{-}2.5}$ at ALS showed peaks with winds out of the west, the direction of the gravel pit and I-76, and with winds from the southwest. $PM_{10\text{-}2.5}$ at EDI had increased concentrations with winds coming from the northeast and secondarily from the southeast. Possible $PM_{10\text{-}2.5}$ sources near EDI include the intersection of I-70 and I-25 2 km to the northeast and I-25 2.5 km to the southeast. $PM_{10\text{-}2.5}$ at CAMP displayed a primary peak with wind from the north-northeast, and secondary peaks with winds from the east, southwest, and northwest. CAMP is located in downtown Denver with intersections within 20 m of the monitoring site to the north, south, and west, and major one-way street directly to the east. The wind direction NPR also suggests the importance of local traffic for $PM_{10-2.5}$ concentrations at DMAS, displaying a peak with winds from the northeast, the direction of I-25 less than half a kilometer away.

$PM_{2.5}$ at ALS peaked with winds from the southwest, the direction of the urban-industrial area between ALS and downtown Denver. Because of the relative location of the Denver monitoring sites, this area north of downtown Denver could also be a "source" region contributing to elevated concentrations of both $PM_{10-2.5}$ and $PM_{2.5}$ with winds from the north for CAMP and DMAS and from the NE for EDI. DMAS is also located in close proximity to I-25, which curves around the east side of the property from north to south, and could contribute to the elevated $PM_{2.5}$ concentrations observed with winds from both the north-northeast and south-southeast directions.

4 Conclusions

The CCRUSH study characterized $PM_{10-2.5}$, $PM_{2.5}$, $SVM_{2.5}$, and $SVM_{10-2.5}$ mass concentrations in urban and rural communities in northeastern Colorado. The CCRUSH data are being used in ongoing epidemiologic studies investigating associations between coarse PM concentrations and health responses in northeastern Colorado. The measurements presented here show that traffic influenced sites in Denver had the highest $PM_{10-2.5}$ concentrations and $PM_{10-2.5}/PM_{10}$ ratios. The CAMP site in downtown Denver had the highest $PM_{10-2.5}$ concentrations, whereas $PM_{2.5}$ concentrations were highest at DMAS and ALS, two monitoring sites located near interstate highways. Average $PM_{10-2.5}$ concentrations at CAMP were about twice as high as those at the residential sites in Denver and Greeley. In contrast, the highest average $PM_{2.5}$ concentration at DMAS was only about 30% higher than the lowest value, which was found at EDI. While $SVM_{2.5}$ ranged from 26 to 29% of the total $PM_{2.5}$ mass, the highest average $SVM_{10-2.5}$ concentration at ALS made up just 1% of the $PM_{10-2.5}$ mass.

Peak monthly median $PM_{10-2.5}$ concentrations generally occurred in summer and fall, reflecting relatively dry conditions during those seasons. $PM_{10-2.5}$ concentrations demonstrated one or two diurnal peaks, corresponding to morning and/or afternoon traffic peaks. Concentrations of $PM_{2.5}$ and $SVM_{2.5}$ shared similar seasonal trends. Along with NO and CO concentrations, they peaked in winter when periodic temperature inversions occurred. Daily average concentrations of $PM_{2.5}$ and $SVM_{2.5}$ were correlated. They showed different diurnal trends, however, with $PM_{2.5}$ peaking on weekday mornings and $SVM_{2.5}$ at about noon. This pattern suggests photolysis-driven atmospheric chemistry has a stronger influence on $SVM_{2.5}$ than on $PM_{2.5}$ as a whole. Clements et al. (2013) discussed the need to account for $SVM_{2.5}$ to correct volatile mass loss from TEOM measurements, which is the function of the FDMS system. Beyond incorporating this correction, researchers and air quality managers might want to separately track $SVM_{2.5}$ concentrations to gain insight into the behavior of this semi-volatile fraction.

Pairwise correlation coefficients for daily average $PM_{10-2.5}$ concentrations between the MAP site in Greeley and the Denver sites were higher than those for $PM_{2.5}$. The relatively high correlations for $PM_{10-2.5}$ may be due to sites across the region having similar influence of synoptic scale meteorology, or to different sites having similar day-to-day patterns in nearby source activity. Within Denver, however, concentrations of $PM_{10-2.5}$ were more heterogeneous than those for $PM_{2.5}$. As suggested by Wilson et al. (2005) the greater heterogeneity in $PM_{10-2.5}$ concentrations would contribute to greater exposure estimation error for urban-scale epidemiologic studies of $PM_{10-2.5}$ health effects, compared to those for $PM_{2.5}$.

As expected, $PM_{10-2.5}$ concentrations generally declined with increasing moisture levels, indicated by RH and soil moisture. $PM_{2.5}$ and $PM_{10-2.5}$ concentrations displayed contrasting relationships with wind speed. $PM_{2.5}$ concentrations generally decreased as wind speeds increased, reflecting the effect of greater dilution at higher wind speeds. $PM_{10-2.5}$ concentrations at traffic-influenced sites increased with wind speeds above 3 m s^{-1}. Wind speed appeared to have less influence on $PM_{10-2.5}$ at EDI and MAP, possibly because these sites were further than the others from major sources such as roadways or gravel operations. In general, the relationships between soil and road dust resuspension, moisture and soil crust state are not well understood, and warrant further research to help in modeling dust emissions (Kok et al., 2014; Klose et al., 2014; Haustein et al., 2015).

Nonparametric regression with wind direction points to the Front Range urban corridor as a source area for relatively high $PM_{2.5}$ in Greeley, but not for $PM_{10-2.5}$. Relatively high $PM_{10-2.5}$ concentrations are seen at MAP when winds are from the east, the direction of a developed part of town as well as two cattle feedlots. All of the Denver sites show increased $PM_{10-2.5}$ concentrations when major traffic corridors and the industrial area in northeast Denver are upwind. Efforts to reduce concentrations of $PM_{10-2.5}$ would be aided by research into means of reducing emissions from heavily traveled roadways, including vehicle and road wear and re-suspension of deposited materials.

Acknowledgements

The CCRUSH study is funded by the National Center for Environmental Research (NCER) of the United States Environmental Protection Agency (EPA) under grant number R833744. We wish to thank and acknowledge the help provided from the following people: Sherri Hunt (EPA), Ricardo Piedrahita (CU), John Ortega (NCAR/CU), Allison Moore (CU), Lisa Coco (University of Northern Colorado), Dan Welsh (University of Northern Colorado), Debbie Bowe (Thermo Scientific), Pat McGraw (CDPHE), Bradley Rink (CDPHE), Tiffany Duhl (CU, monitoring site map), Greg Philp (Weld County School District 6), Phil Brewer (Weld County Public Health), and all custodial and front office staff at schools used as monitoring sites.

References

Adar, S., Filigrana, P., Clements, N., Peel, J.L. Ambient Coarse Particulate Matter and Human Health: A Systematic Review and Meta-Analysis. Curr. Environ. Health Rep. 1(3), 258-274, 2014.

Amato, F., Schaap, M., Denier van der Gon, H.A.C., Pandolfi, M., Alastuey, A., Keuken, M., Querol, X. Short-term variability of mineral dust, metals and carbon emission from road dust resuspension. Atmos. Environ. 74, 134-140, 2013.

Amato, F., Alastuey, A., de la Rosa, J., Gonzalez Castanedo, Y., Sanchez de la Campa, A.M., Pandolfi, M., Lozano, A., Contreras Gonzalez, J., Querol, X. Trends of road dust emissions contributions on ambient air particulate levels at rural, urban and industrial sites in southern Spain. Atmos. Chem. Phys. 14, 3533-3544, 2014.

Barmpadimos, I., Keller, J., Oderbolz, D., Hueglin, C., Prevot, A.S.H. One decade of parallel fine ($PM_{2.5}$) and coarse (PM_{10}-$PM_{2.5}$) particulate matter measurements in Europe: trends and variability. Atmos. Chem. Phys. 12, 3189-3203, 2012.

Bowers, R.M., Clements, N., Emerson, J.B., Wiedinmyer, C., Hannigan, M.P., Fierer, N. Seasonal Variability in Bacterial and Fungal Diversity of the Near-Surface Atmosphere. Environ. Sci. Technol. 47, 12097-12106, 2013.

Brunekreef, B., Forsberg, B. Epidemiological evidence of effects of coarse ambient particles on health, Eur. Respir. J. 26, 309-318, 2005.

Charron, A., Harrison, R.M. Fine ($PM_{2.5}$) and Coarse ($PM_{2.5-10}$) Particulate Matter on A Heavily Trafficked London Highway: Sources and Processes. Environ. Sci. Technol. 39, 7768-7776, 2005.

Cheung, K., Daher, N., Kam, W., Shafer, M.M., Ning, Z., Schauer, J.J., Sioutas, C. Spatial and temporal variation of chemical composition and mass closure of ambient coarse particulate matter ($PM_{10-2.5}$) in the Los Angeles area. Atmos. Environ. 45, 2651-2662, 2011.

Cheung, K., Olson, M.R., Shelton, B., Schauer, J.J., Sioutas, C. Seasonal and spatial variations of individual organic compounds of coarse particulate matter in the Los Angeles Basin. Atmos. Environ. 59, 1-10, 2012.

Clements, N., Piedrahita, R., Ortega, J., Peel, J.L., Hannigan, M., Miller, S.L., Milford, J.B., Characterization and Nonparametric Regression of Rural and Urban Coarse Particulate Matter Mass Concentrations in Northeastern Colorado, Aerosol Sci. Tech. 46(1), 108-123, 2012.

Clements, N., Milford, J.B., Miller, S.L., Navidi, W., Peel, J.L., Hannigan, M.P. Errors in Coarse Particulate Matter ($PM_{10-2.5}$) Mass Concentrations and Spatiotemporal Characteristics when Using Subtraction Estimation Methods, J. Air Waste Manage., 63(12), 1386-1398, 2013.

Clements, N. The CCRUSH Study: Characterization of Coarse and Fine Particulate Matter in Northeastern Colorado. PhD. Dissertation, University of Colorado Boulder, 2013.

Clements, N., Eav, J., Xie, M., Hannigan, M.P., Miller, S.L., Navidi, W., Peel, J.L., Schauer, J.J., Shafer, M., Milford, J.B. Concentrations and Source Insights for Trace Elements in Fine and Coarse Particulate Matter in Northeastern Colorado, Atmos. Environ. 89, 373-381, 2014.

Dutton, S.J., Vedal, S., Piedrahita, R., Milford, J.B., Miller, S.L., Hannigan, M.P. Source apportionment using positive matrix factorization on daily measurements of inorganic and organic speciated $PM_{2.5}$. Atmos. Environ. 44, 2731-2741, 2010.

Favez, O., Cachier, H., Sciare, J., Le Moullec, Y. Characterization and contribution to $PM_{2.5}$ of semi-volatile aerosols in Paris (France), Atmos. Environ. 41, 7969-7976, 2007.

Grover, B.D., Eatough, N.L., Eatough, D.J., Chow, J.C., Watson, J.G., Ambs, J.L., Meyer, M.B., Hopke, P.K., Al-Horr, R., Later, D.W., Wilson, W.E. Measurement of Both Nonvolatile and Semi-Volatile Fractions of Fine Particulate Matter in Fresno, CA, Aerosol Sci. Tech. 40, 811-826, 2006.

Harrison, R.M., Yin, J., Mark, D., Stedman, J., Appleby, R.S., Booker, J., Moorcroft, S. Studies of the coarse particles (2.5-10 μm) component in UK urban atmospheres. Atmos. Environ. 35, 3667-3679, 2001.

Harrison, R.M., Jones, A.M., Gietl, J., Yin, J., Green, D.C. Estimation of the Contributions of Brake Dust, Tire Wear, and Resuspension to Nonexhaust Traffic Particles Derived from Atmospheric Measurements, Environ. Sci. Technol. 46, 6523-6529, 2012.

Haustein, K., Washington, R., King, J., Wiggs, G., Thomas, D.S.G., Eckardt, F.D., Bryant, R.G., Menut, L. Testing the performance of state-of-the-art dust emission schemes using DO4Models field data. Geosci. Model Dev. 8, 341-362, 2015.

Henry, R.C., Chang, Y.-S., Spiegelman, C.H. Locating nearby sources of air pollution by nonparametric regression of atmospheric concentration on wind direction, Atmos. Environ. 36, 2237-2244, 2002.

Hering, S., Fine, P.M., Sioutas, C., Jaques, P.A., Ambs, J.L., Hogrefe, O., Demerjian, K. L. Field assessment of the dynamics of particulate nitrate vaporization using differential TEOM® and automated nitrate monitors. Atmos. Environ. 38, 5183-5192, 2004.

Hiranuma, N., Brooks, S.D., Gramann, J., Auvermann, B.W. High concentrations of coarse particles emitted from a cattle feeding operation. Atmos. Chem. Phys. 11, 8809-8823, 2011.

Huffman, J.A., Prenni, A.J., DeMott, P.J., Pohlker, C., Mason, R.H., Robinson, N.H., Frohlich-Nowoisky, J., Tobo, Y., Despres, V.R., Garcia, E., Gochis, D.J., Harris, E., Muller-Germann, I., Ruzene, C., Schmer, B., Sinha, B., Day, D.A., Andreae, M.O., Jimenez, J.L., Gallagher, M., Kreidenweis, S.M., Bertram, A.K., Poschl, U. High Concentrations of biological aerosol particles and ice nuclei during and after rain. Atmos. Chem. Phys. 13, 6151-6164, 2013.

Kavouras, I. G., Etyemezian, V., Xu, J., DuBois, D. W., Green, M., and Pitchford, M.: Assessment of the local windblown component of dust in the western United States, J. Geophys. Res., 112, D08211, doi:10.1029/2006JD007832, 2007.

Kim, D. and Ramanathan, V.: Solar radiation budget and radiative forcing due to aerosols and clouds, J. Geophys. Res., 113, D02203, doi:10.1029/2007JD008434, 2008.

Kim, H., Choi, M. Impact of Soil Moisture on Dust Outbreaks in East Asia: Using Satellite and Assimilation Data. Geophys. Res. Let. 42(8), 2789-2796, 2015.

Klose, M., Shao, Y., Li, X., Zhang, H., Ishizuka, M., Mikami, M., Leys, J.F. Further development of a parameterization for convective turbulent dust emission and evaluation based on field observations. J. Geophys. Res.-Atmos. 119(17), 10441-10457, 2014.

Kok, J.F., Mahowald, N.M., Fratini, G., Gillies, J.A., Ishizuka, M., Leys, J.F., Mikami, M., Park, M.-S., Park, S.-U., Van Pelt, R.S., Zobeck, T.M. An improved dust emission model – Part 1: Model description and comparison against measurements. Atmos. Chem. Phys. 14, 13023-13041, 2014.

Kumar, P., Hopke, P.K., Raja, S., Casuccio, G., Lersch, T.L., West, R.R. Characterization and heterogeneity of coarse particles across an urban area, Atmos. Environ. 46, 446-459, 2012.

Lee, T., Yu, X.-Y., Ayres, B., Kreidenweis, S.M., Malm, W.C., Collett, J.L.Jr. Observations of fine and coarse particle nitrate at several rural locations in the United States. Atmos. Environ. 42, 2720-2732, 2008.

Li, R., Wiedinmyer, C., Baker, K.R., Hannigan, M.P. Characterization of coarse particulate matter in the western United States: a comparison between observation and modeling. Atmos. Chem. Phys. 13, 1311-1327, 2013.

Lin, L.I.-K. A Concordance Correlation Coefficient to Evaluate Reproducibility, Biometrics 45(1), 255-268, 1989.

Liu, Y.-J., Harrison, R.M. Properties of coarse particles in the atmosphere of the United Kingdom. Atmos. Environ. 45, 3267-3276, 2011.

Malm, W.C., Pitchford, M.L., McDade, C., Ashbaugh, L.L. Coarse particle speciation at selected locations in the rural continental United States, Atmos. Environ. 41, 2225-2239, 2007.

Minguillon, Maria Cruz, Campos, Arturo Alberto, Cardenas, Beatriz, Blanco, Salvador, Molina, Luisa T., Querol, Xavier. Mass concentration, composition and sources of fine and coarse particulate matter in Tijuana, Mexico, during Cal-Mex campaign. Atmos. Environ. 88, 320-329, 2014.

Moore, K.F., Verma, V., Minguillon, M.C., Sioutas, C. Inter- and Intra-Community Variability in Continuous Coarse Particulate Matter (PM10-2.5) Concentrations in the Los Angeles Area. Aerosol Sci. Tech. 44(7), 526-540, 2010.

O'Sullivan, D., Murray, B. J., Ross, J. F., Whale, T. F., Price, H. C., Atkinson, J. D., Umo, N. S. and Webb, M. E.: The relevance of nanoscale biological fragments for ice nucleation in clouds, Sci. Rep., 5, 8082, doi:10.1038/srep08082, 2015.

Pakbin, P., Hudda, N., Cheung, K.L., Moore, K.F., Sioutas, C. Spatial and Temporal Variability of Coarse (PM10-2.5) Particulate Matter Concentrations in the Los Angeles Area. Aerosol Sci. Tech. 44(7), 514-525, 2010.

Pakbin, P., Ning, Z., Shafer, M.M., Schauer, J.J., Constantinos, S. Seasonal and Spatial Coarse Particle Elemental Concentrations in the Los Angeles Area. Aerosol Sci. Tech. 45(8), 949-963, 2011.

Sawvel, Eric J., Willis, Robert, West, Roger R., Casuccio, Gary S., Norris, Gary, Kumar, Naresh, Hammond, Davyda, Peters, Thomas M. Passive sampling to capture the spatial variability of coarse particles by composition in Cleveland, OH. Atmos. Environ. 105, 61-69, 2015.

Sciare, J., Cachier, H., Sarda-Esteve, R., Yu, T., and Wang, X.: Semi-volatile aerosol in Beijing (R. P. China): characterization and influence on various PM2.5 measurements, J. Geophys. Res., 112, D18202, doi:10.1029/2006JD007448, 2007.

Seinfeld, J.H., Spyros, P.N. Atmospheric Chemistry and Physics - From Air Pollution to Climate Change, 2nd Edition, John Wily & Sons, 2006.

Stevens, B., Feingold, G. Untangling aerosol effects on clouds and precipitation in a buffered system, Nature 461, 607-613, 2009.

Thermo Scientific: TEOM 1405-DF: Dichotomous Ambient Particulate Monitor with FDMS Option, 42-010815 Revision, A.003, Thermo Scientific, Franklin, MA, 2009.

US Bureau of the Census: Annual Estimates of the Resident Population for Counties of Colorado: April 1, 2010 to July 1, 2011. Prepared by the United States Census Bureau, Population Division, available at: http://www.census.gov/popest/data/counties/totals/2011/tables/CO-EST2011-01-08.csv (last access: December 2014), 2012.

U.S. Department of Agriculture. *2012 Census Volume 1, Chapter 2: County Level Data, Colorado Volume 1, Complete Report.* Prepared by the United States Department of Agriculture, Washington, DC, 2012.

U.S. EPA. *US EPA Air Quality Criteria for Particulate Matter (Final Report, Oct, 2004)*. U.S. Environmental Protection Agency, Washington, DC, EPA 600/P-99/002aF-bF, 2004.

Usher, C.R., Michel, A.E., Grassian, V.H. Reactions on Mineral Dust. Chem. Rev. 103, 4883-4939, 2003.

Wang, G., Kawamura, K., Xie, M., Hu, S., Cao, J., An, Z., Waston, J.G., Chow, J.C. Organic Molecular Compositions and Size Distributions of Chinese Summer and Autumn Aerosols from Nanjing: Characteristic Haze Event Caused by Wheat Straw Burning. Environ. Sci. Technol. 43, 6493-6499, 2009.

Wang, M., Ghan, S., Ovchinnikov, M., Liu, X., Easter, R., Kassianov, E., Qian, Y., Morrison, H. Aerosol indirect effects in a multi-scale aerosol-climate model PNNL-MMF, Atmos. Chem. Phys. 11, 5431-5455, 2011.

Wilson, J.G., Kingham, S., Pearce, J., Sturman, A.P. A review of intraurban variations in particulate air pollution: Implications for epidemiological research, Atmos. Environ. 39, 6444-6462, 2005.

Xie, M., Piedrahita, R., Dutton, S.J., Milford, J.B., Hemann, J.G., Peel., J.L., Miller, S.L., Kim, S.-Y., Vedal, S., Sheppard, L., Hannigan, M.P. Positive matrix factorization of a 32-month series of daily $PM_{2.5}$ speciated data with incorporation of temperature stratification. Atmos. Environ. 65, 11-20, 2013.

Table 1. Summary description of the CCRUSH and CDPHE particulate monitoring sites.

Monitoring Site	ALS (CCRUSH)	EDI (CCRUSH)	CAMP (CDPHE)	DMAS (CDPHE)	MAP (CCRUSH)	MCA (CCRUSH)
City	Denver	Denver	Denver	Denver	Greeley	Greeley
Coordinates	39.83N 104.94W	39.76N 105.04W	39.75N 104.99W	39.70N 105.00W	40.42N 104.71W	40.43N 104.77W
Start Date	1/26/2009	1/8/2009	1/1/2009	1/1/2009	1/16/2009	1/1/2009
End Date	9/29/2011	3/1/2012	4/30/2012	4/30/2012	2/2/2012	6/19/2009
Site Description	Industrial-Residential	Urban-Residential	Urban-Roadside	Urban-Roadside	Rural-Residential	Rural-Residential
Instruments	TEOM 1405-DF (FDMS)	TEOM 1405-DF (FDMS)	TEOM 1400a (FDMS); TEOM 1400ab (no FDMS)	TEOM 1400a (FDMS); TEOM 1400ab (no FDMS)	TEOM 1405-DF (FDMS)	TEOM 1405-DF (FDMS)
Inlet Height (m)	6	9	6	5	9	10.5

Table 2. Summary statistics of particulate matter concentrations during the CCRUSH campaign. Statistics are for daily averages except where indicated.

Monitoring Site (City, Site Type)	**ALS (Denver, Industrial-Residential)**					**EDI (Denver, Urban-Residential)**				
Particulate Fraction	$PM_{2.5}$	$SVM_{2.5}$	$PM_{10-2.5}$	$SVM_{10-2.5}$	$PM_{10-2.5}$/ PM_{10}	$PM_{2.5}$	$SVM_{2.5}$	$PM_{10-2.5}$	$SVM_{10-2.5}$	$PM_{10-2.5}$/ PM_{10}
Mean (St. Dev., μg/m^3)	9.02 (4.64)	2.32 (1.50)	15.30 (10.36)	0.20 (0.30)	0.59 (0.18)	7.66 (5.33)	2.05 (1.91)	8.02 (4.85)	0.02 (0.25)	0.51 (0.21)
Median (μg/m^3)	8.07	2.08	13.37	0.16	0.62	6.55	1.81	7.17	0.01	0.53
5^{th}/95^{th} Per. (μg/m^3)	3.90/ 16.90	0.50/ 5.29	2.02/ 35.74	-0.20/ 0.72	0.23/ 0.81	2.14/ 16.92	-0.28/ 5.16	1.61/ 17.20	-0.35/ 0.44	0.20/ 0.77
Daily COV[a] (Hourly COV)	0.51 (0.82)	0.65 (1.56)	0.68 (1.20)	1.53 (5.83)	0.31 (-)	0.70 (1.16)	0.93 (2.37)	0.61 (0.96)	13.18 (37.50)	0.40
N (% Complete)	755 (76%)					747 (65%)				
Monitoring Site (City, Site Type)	**CAMP (Denver, Urban-Roadside)**					**DMAS (Denver, Urban-Roadside)**				
Particulate Fraction	$PM_{2.5}$	$SVM_{2.5}$[b]	$PM_{10-2.5}$[c]	$SVM_{10-2.5}$	$PM_{10-2.5}$/ PM_{10}	$PM_{2.5}$	$SVM_{2.5}$[b]	$PM_{10-2.5}$[c]	$SVM_{10-2.5}$	$PM_{10-2.5}$/ PM_{10}
Mean (St. Dev., μg/m^3)	7.97 (4.40)	1.42 (1.08)	19.71 (10.53)	-	0.70 (0.15)	10.15 (4.51)	2.72 (1.14)	14.60 (8.20)	-	0.56 (0.19)
Median (μg/m^3)	7.14	1.22	18.09	-	0.74	9.30	2.50	13.89	-	0.61
5^{th}/95^{th} Per. (μg/m^3)	3.01/ 16.59	0.20/ 3.54	5.22/ 38.88	-	0.38/ 0.86	4.95/ 18.18	1.40/ 4.74	2.62/ 28.63	-	0.20/ 0.77
Daily COV (Hourly COV)	0.55 (0.81)	0.76 (-)	0.53 (1.07)	-	0.21	0.44 (0.63)	0.42 (-)	0.56 (1.34)	-	0.34
N (% Complete)	1121 (92%)	1121 (92%)	503 (90%)	-	503 (90%)	1097 (90%)	1097 (90%)	980 (81%)	-	980 (81%)
Monitoring Site (City, Site Type)	**MAP (Greeley, Rural-Residential)**					**MCA (Greeley, Rural-Residential)**				
Particulate Fraction	$PM_{2.5}$	$SVM_{2.5}$	$PM_{10-2.5}$	$SVM_{10-2.5}$[d]	$PM_{10-2.5}$/ PM_{10}	$PM_{2.5}$	$SVM_{2.5}$	$PM_{10-2.5}$	$SVM_{10-2.5}$	$PM_{10-2.5}$/ PM_{10}
Mean (St. Dev., μg/m^3)	8.15 (4.79)	2.39 (1.80)	10.34 (7.11)	0.05 (0.38)	0.53 (0.20)	8.68 (4.29)	2.58 (1.54)	9.87 (7.74)	-0.06 (0.24)	0.49 (0.18)
Median (μg/m^3)	7.13	2.22	9.17	0.05	0.56	7.71	2.22	7.76	-0.05	0.50
5^{th}/95^{th} Per. (μg/m^3)	2.60/ 17.64	0.10/ 5.41	1.63/ 22.89	-0.54/ 0.62	0.19/ 0.78	4.45/ 15.43	0.75/ 4.87	1.69/ 23.97	-0.39/ 0.29	0.15/ 0.76
Daily COV (Hourly COV)	0.59 (0.91)	0.75 (1.89)	0.69 (1.09)	7.68 (36.33)	0.37	0.49 (0.86)	0.60 (1.46)	0.78 (1.28)	4.19 (13.21)	0.37
N (% Complete)	822, $SVM_{10-2.5}$: 788 (74%, $SVM_{10-2.5}$: 71%)					168 (99%)				

[a] Defined abbreviations: Standard Deviation (St. Dev.), Coefficient of Variation (COV), Percentile (Per.), and Sample Number (N)
[b] Estimated using the regression models presented in Clements et al. (2013)
[c] Corrected subtraction-method errors using the method of Clements et al. (2013)
[d] MAP $PM_{10-2.5}$ semi-volatile concentrations were not available from 8/13/2009 to 9/18/2009, $PM_{10-2.5}$ non-volatile concentrations were used to estimate total $PM_{10-2.5}$ for this period

Table 3. Pearson's correlation coefficient (ρ) values are listed below the diagonal, concordance correlation coefficient (CCC) values above the diagonal, and bias correction factor (C_b) values in parentheses for spatial comparisons of daily averaged $PM_{2.5}$, $PM_{10\text{-}2.5}$, and $SVM_{2.5}$.

ρ\CCC *(C_b)*		**$PM_{2.5}$**					**$PM_{10\text{-}2.5}$**					**$SVM_{2.5}$**		
		ALS	**EDI**	**CAMP**	**DMAS**	**MAP**	**ALS**	**EDI**	**CAMP**	**DMAS**	**MAP**	**ALS**	**EDI**	**MAP**
$PM_{2.5}$	**ALS**	**1.00**	0.62 *(0.96)*	0.82 *(0.98)*	0.71 *(0.96)*	0.56 *(0.92)*	0.10	0.28	-0.01	0.08	0.03	0.16	0.09	0.06
	EDI	0.65	**1.00**	0.72 *(0.96)*	0.66 *(0.85)*	0.34 *(0.99)*	-0.04	0.22	-0.08	-0.07	-0.06	0.12	0.25	0.08
	CAMP	0.83	0.75	**1.00**	0.86 *(0.94)*	0.37 *(0.94)*	0.12	0.26	0.05	0.05	0.07	0.12	0.22	0.11
	DMAS	0.74	0.78	0.92	**1.00**	0.37 *(0.94)*	0.03	0.21	0.01	-0.01	-0.05	0.08	0.11	0.04
	MAP	0.61	0.34	0.39	0.41	**1.00**	0.05	0.20	-0.01	0.06	0.14	0.13	0.05	0.22
$PM_{10\text{-}2.5}$	**ALS**	0.17	-0.10	0.19	0.06	0.11	**1.00**	0.40 *(0.57)*	0.38 *(0.65)*	0.68 *(0.94)*	0.57 *(0.80)*	-0.02	-0.03	-0.01
	EDI	0.28	0.22	0.26	0.24	0.20	0.70	**1.00**	0.20 *(0.33)*	0.43 *(0.62)*	0.58 *(0.84)*	-0.02	0.00	0.01
	CAMP	-0.03	-0.18	0.13	0.02	-0.02	0.59	0.62	**1.00**	0.66 *(0.83)*	0.28 *(0.60)*	-0.01	-0.02	0.00
	DMAS	0.13	-0.12	0.08	-0.02	0.09	0.72	0.70	0.79	**1.00**	0.60 *(0.90)*	-0.01	-0.03	0.00
	MAP	0.04	-0.08	0.09	-0.06	0.16	0.70	0.69	0.47	0.67	**1.00**	-0.04	-0.03	0.00
$SVM_{2.5}$	**ALS**	0.77	0.50	0.54	0.53	0.47	-0.14	-0.08	-0.16	-0.14	-0.20	**1.00**	0.53 *(0.99)*	0.37 *(0.99)*
	EDI	0.45	0.80	0.61	0.59	0.21	-0.24	0.01	-0.20	-0.19	-0.14	0.53	**1.00**	0.25 *(0.96)*
	MAP	0.30	0.25	0.28	0.23	0.77	-0.07	0.03	-0.01	0.00	0.01	0.37	0.26	**1.00**

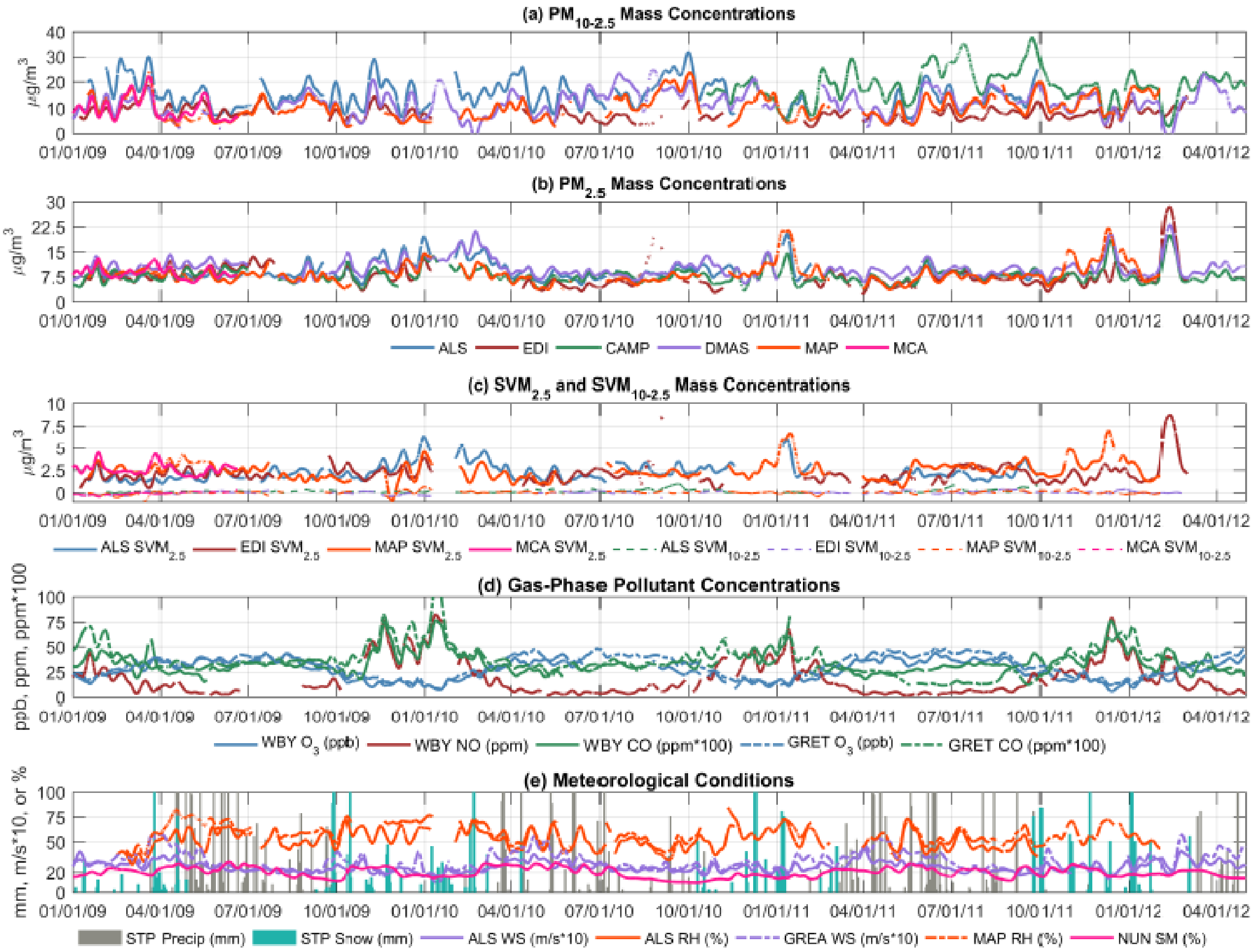

Figure 1. Smoothed (Δθ=3 hours) time series of hourly average (a) $PM_{10\text{-}2.5}$ mass concentrations, (b) $PM_{2.5}$ mass concentrations, (c) $SVM_{2.5}$ and $SVM_{10\text{-}2.5}$ mass concentrations, (d) gas-phase pollutant concentrations, and (e) meteorological conditions (WS and SM stand for wind speed and soil moisture, respectively, precipitation and snowfall data sets are daily totals with no smoothing).

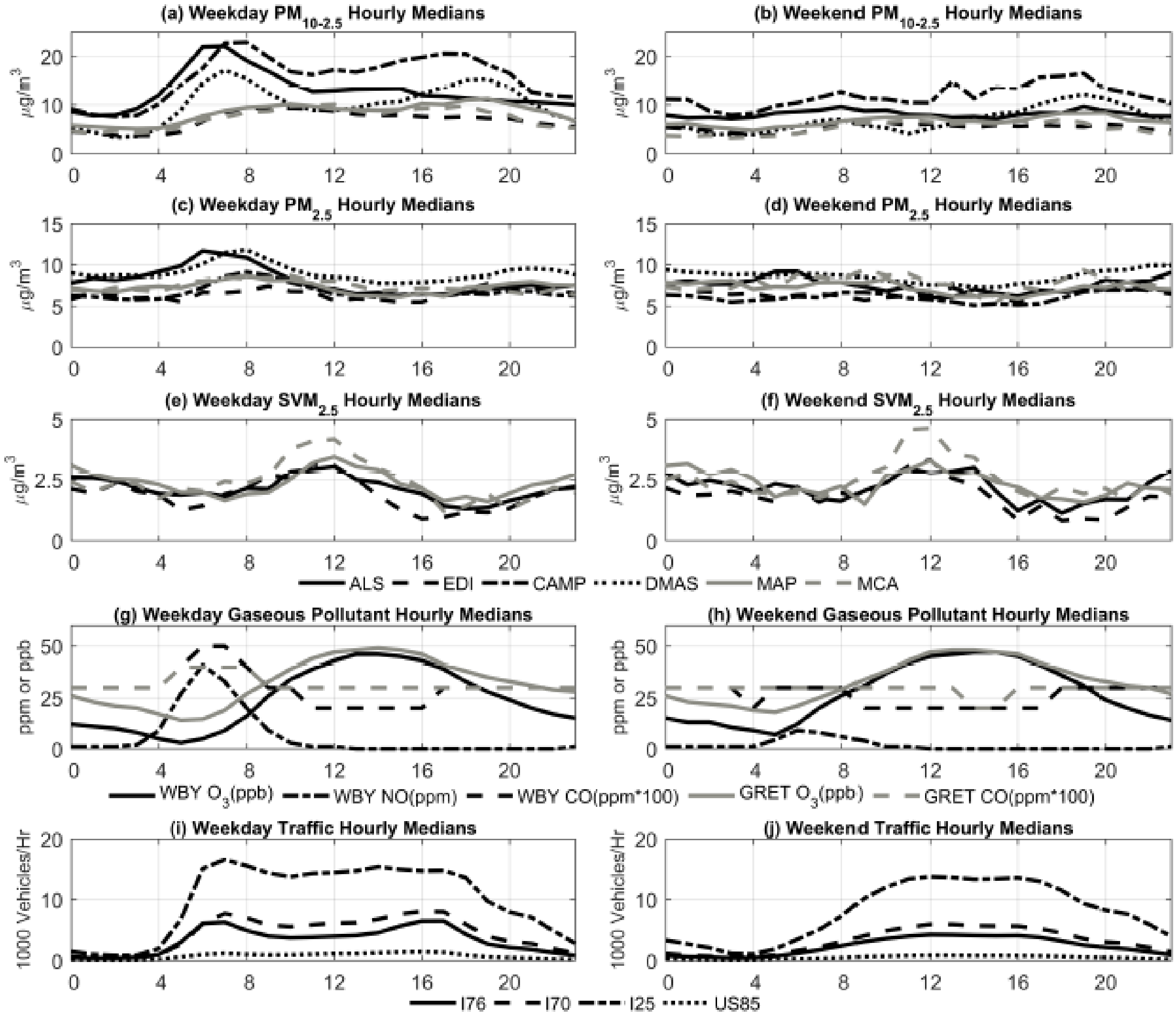

Figure 2. Diurnal trends (time-of-day medians) of (a) $PM_{10-2.5}$ on weekdays, (b) $PM_{10-2.5}$ on weekends, (c) $PM_{2.5}$ on weekdays, (d) $PM_{2.5}$ on weekends, (e) $SVM_{2.5}$ on weekdays, (f) $SVM_{2.5}$ on weekends, (g) weekday gas-phase pollutants, (h) weekend gas-phase pollutants, (i) weekday traffic volumes, and (j) weekend traffic volumes.

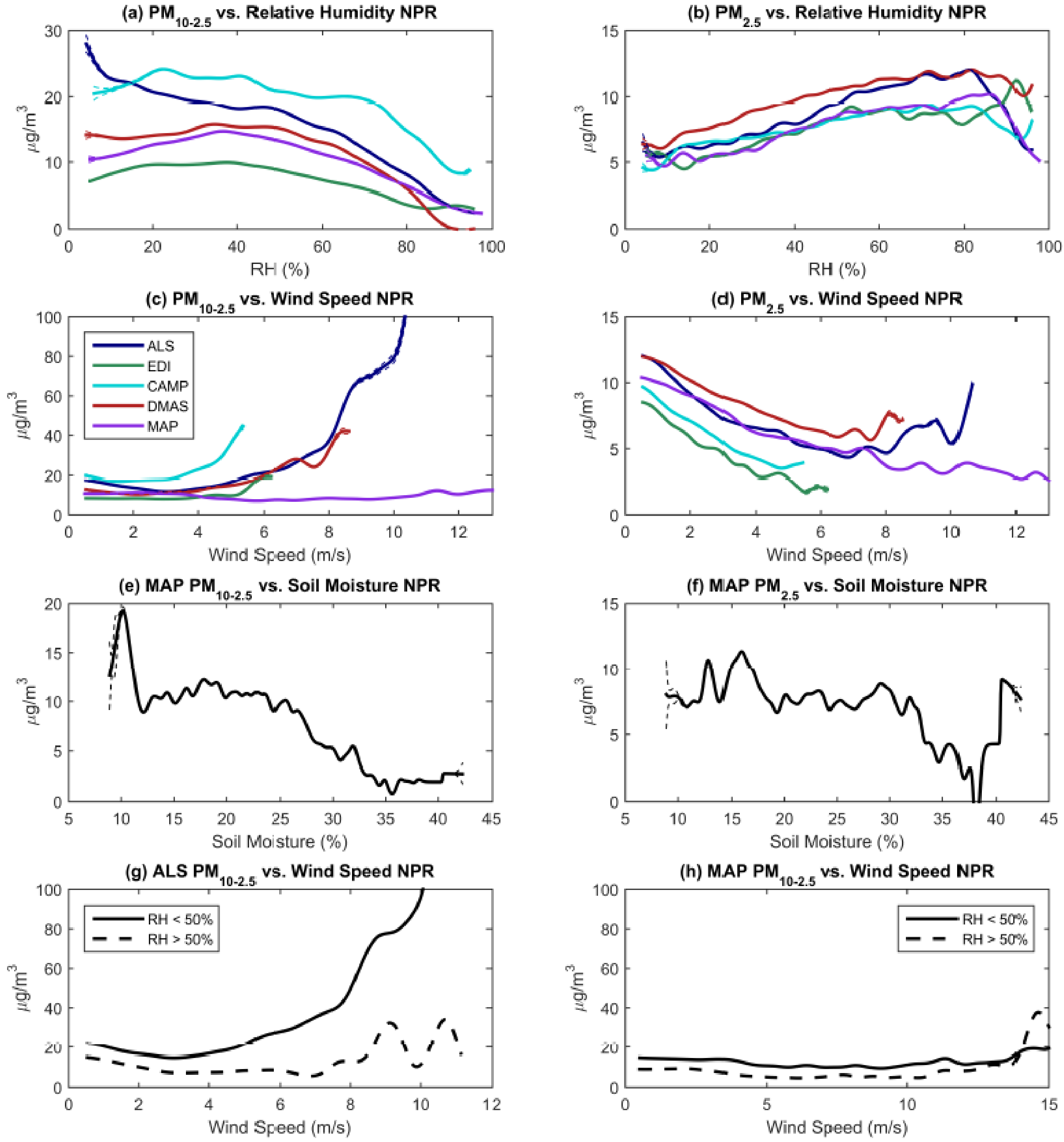

Figure 3. Expected value of pollutant concentrations (dashed lines are 95% confidence intervals) based on nonparametric regression (NPR) of: (a) $PM_{10\text{-}2.5}$ versus RH; (b) $PM_{2.5}$ versus RH; (c) $PM_{10\text{-}2.5}$ versus wind speed; (d) $PM_{2.5}$ versus wind speed; (e) MAP $PM_{10\text{-}2.5}$ versus soil moisture; (f) MAP $PM_{2.5}$ versus soil moisture; (g) ALS $PM_{10\text{-}2.5}$ versus wind speed with data stratified at 50% RH; and (h) MAP $PM_{10\text{-}2.5}$ versus wind speed with data stratified at 50% RH.

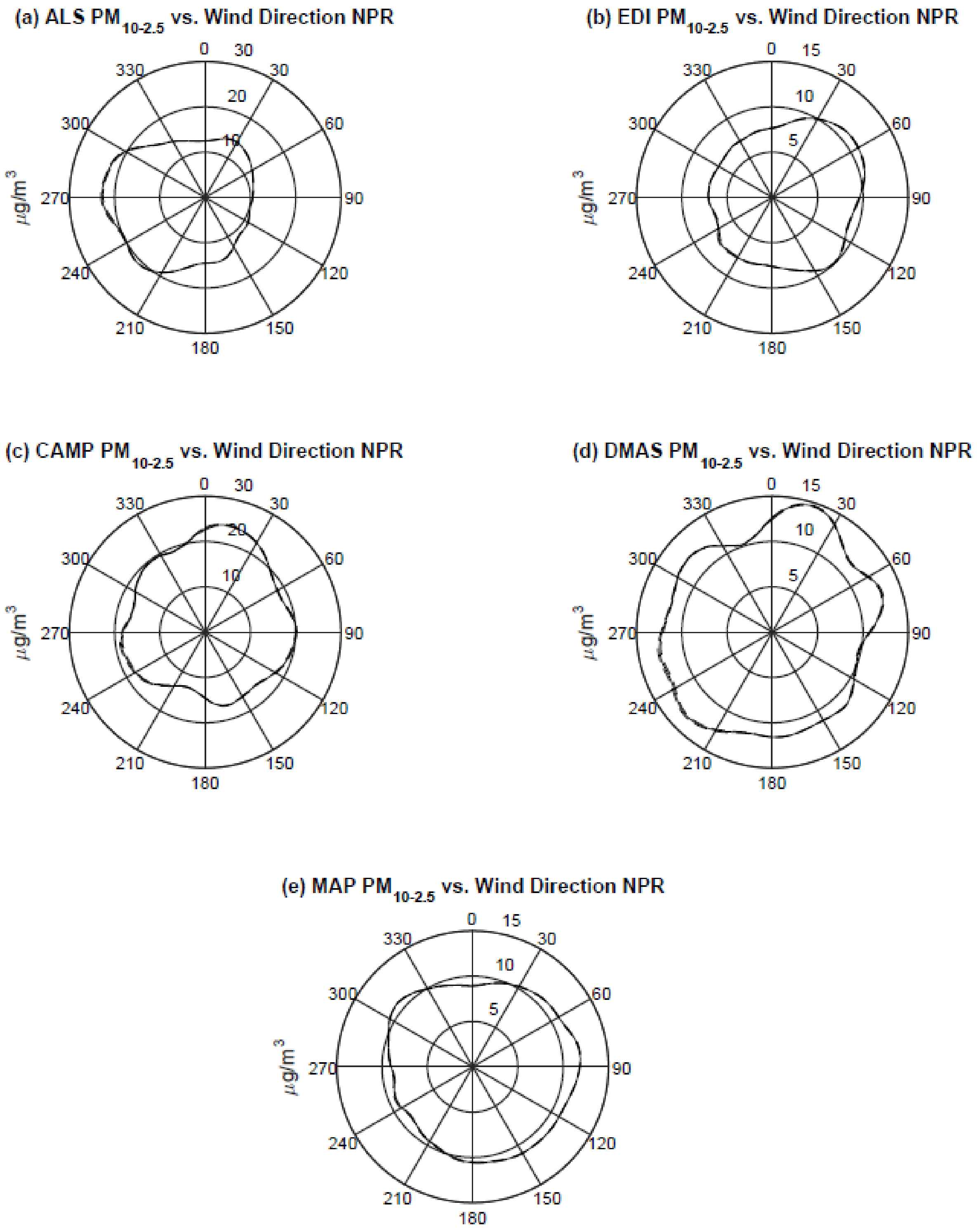

Figure 4. Expected value of $PM_{10-2.5}$ concentrations (dashed lines are 95% confidence intervals) based on nonparametric regression (NPR) against wind direction for (a) ALS, (b) EDI, (c) CAMP, (d) DMAS, and (e) MAP.

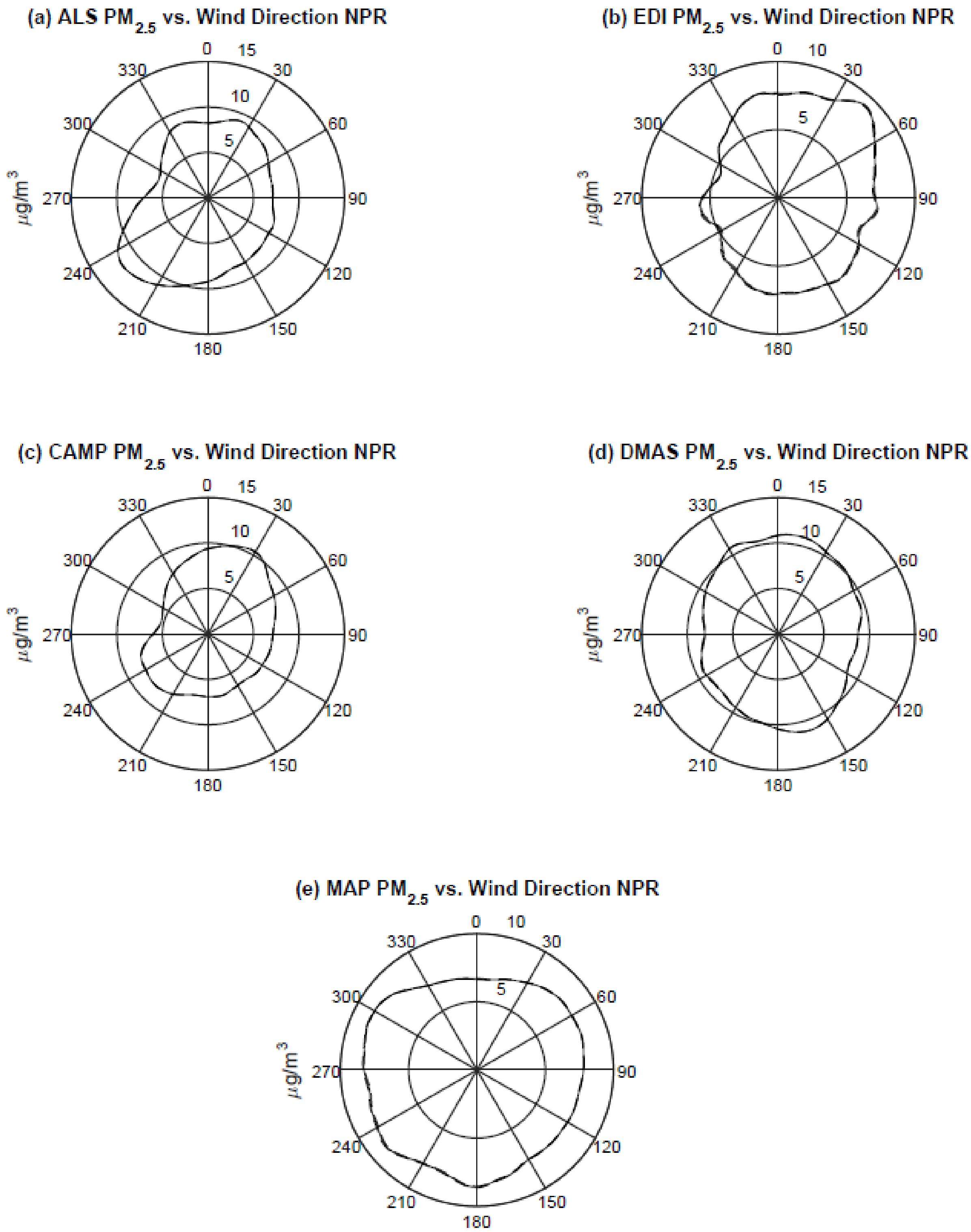

Figure 5. Expected value of $PM_{2.5}$ concentrations (dashed lines are 95% confidence intervals) based on nonparametric regression (NPR) against wind direction for (a) ALS, (b) EDI, (c) CAMP, (d) DMAS, and (e) MAP.